DC Electric Metamaterial Behaviour in Tuned Fused Deposition Modelling Prints

Alexander Dijkshoorn, Thijs Hamstra, Remco Sanders, Stefano Stramigioli, Gijs Krijnen
Robotics and Mechatronics Group, University of Twente, Enschede, the Netherlands
a.p.dijkshoorn@utwente.nl

2021 IEEE Sensors | 978-1-7281-9501-8/21/$31.00 ©2021 IEEE | DOI: 10.1109/SENSORS47087.2021.9639490

***Abstract*—This paper shows the realization of electric metamaterials with Fused Deposition Modelling by tuning the nozzle temperature, bed temperature and extrusion width to achieve anisotropic electrical conduction. The temperatures influence the magnitude of the contact resistance between printed lines, whereas the extrusion width determines the number of contacts per unit length. Electric metamaterials are interesting for sensing, e.g. by concentrating the current to achieve highly sensitive spots. In this work such a concentrator is 3D-printed and its operation is demonstrated through IR thermography and voltage measurements, as well as supported by FEM simulations.**

***Index Terms*—3D-Printing, Fused Deposition Modelling, Electric Metamaterial, Conductive, Anisotropy**

I. Introduction

3D-printing of electrically conductive materials for sensor applications by means of Fused Deposition Modeling (FDM) is an upcoming area of research [1]–[3]. One of the main advantages is that it allows for embedding sensors with electronics in objects in one manufacturing step [4], [5]. On the other hand the FDM process introduces anisotropy due to line-wise and layer-wise manufacturing, e.g. giving rise to anisotropic electrical properties due to the contact resistances between lines and layers [6]–[8]. The printing induced anisotropic properties have e.g. been used for sensing, like constriction-resistive strain sensing [9] and force-dependent impedance sensing [10]. However, the anisotropy also gives rise to metamaterial behaviour, which can be useful for sensors. Metamaterials can serve sensor purposes by enhancing the sensitivity through concentrating the fields used to measure [11], [12] or by cloaking the sensor to prevent perturbing the to-be-measured field [13]. It has been shown that anisotropic, steady-state metamaterials, e.g. for the thermal and electrical domains, can be realized with layered structures of two materials with dissimilar conductivities [14]–[16].

Currently, the fabrication of electric metamaterial structures is achieved by creating resistor networks [12], [17], [18] and by stacking or merging thin layers of materials [13], [14], [19]. In this respect 3D-printing, and especially FDM with its anisotropy due to the structured materials it produces, used as fabrication method for metamaterials can offer advantages in terms of costs, geometric freedom, available materials, lead time and embedding [20]–[22]. Furthermore the infill pattern of (multi-material) FDM with its sub-millimeter resolution is ideally suited to print the repeating, layered structures required for metamaterials [20].

This work was partially developed within the PortWings project, funded by the European Research Council under Grant Agreement No. 787675.

Since realizing metamaterials with FDM is expected to offer an additional tool in the design toolbox for 3D-printing of sensors and conductors, this work studies the fabrication of DC electric metamaterials by means of Fused Deposition Modelling. The effect of several printing parameters on the anisotropic electrical conduction is measured and the findings are used to demonstrate a 3D-printed DC electric metamaterial concentrator. The following sections present the metamaterial theory and show experimental data and simulations to demonstrate the role of the printing parameters and the metamaterial operation.

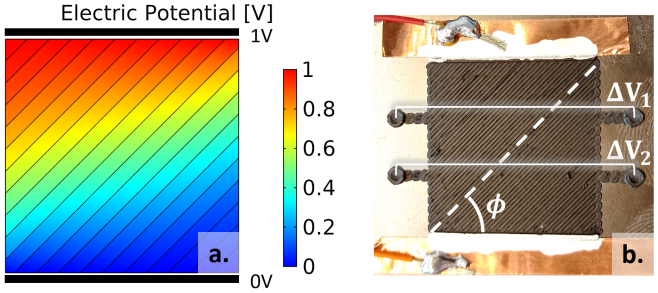

Fig. 1. **a.** FEM simulation of a 3D-printed layer, showing an anisotropic voltage distribution due to contact resistance between lines. **b.** 3D-printed sample with an infill angle of $\phi = 45°$, contacts made of copper tape with silver paint and two pairs of probing points to measure the skewed voltage due to anisotropy at two positions, ΔV_1 and ΔV_2.

II. Theory

Metamaterials can be defined as rationally designed materials with an, often periodic, artificial structure, where the properties are dictated by the structure instead of by the base material [20], [21]. Metamaterials operate in wavelengths greater than the functional building blocks or unit cells of the structure [15].

In this study single 3D-printed sheets with a $45°$ infill pattern are studied, of which a Finite Element Method (FEM) simulation with anisotropic voltage distribution is shown in fig. 1.a. In this case a single material with contact resistance between the printed lines is used to create the anisotropic conduction, instead of the standard method of using two materials with different resistivities. These tiles can be combined in different patterns to achieve different functionalities, e.g. to cloak, to concentrate, to diffuse [16], [23].

Modeling shows that both the orientation of the layers and an additional tuning parameter based on the material properties can be used to change the direction and magnitude of the electric field for an infinite sheet with dual material layers [24]. In the present research the anisotropy is determined by the contact resistance instead of by dual materials. The prints have an in-line resistivity of ρ in $\Omega\,\mathrm{m}$ and a homogenized resistivity of $\rho+\sigma/W_{\text{ext}}$ perpendicular to the printed lines, with σ in $\Omega\,\mathrm{m}^2$ being the contact resistance and W_{ext} the extrusion width. For large σ the current density mainly follows the infill direction, yielding a skewed voltage distribution like in fig. 1.a. The tuning parameter is the anisotropy ratio, defined as the ratio of resistivities in the direction along and the direction normal to the printed lines [25]:

$$\Gamma = \frac{\rho}{\rho + \sigma/W_{\text{ext}}} \tag{1}$$

In case of ideal isotropic conduction $\Gamma = 1$ and for significant anisotropy, with metamaterial properties, $\Gamma \ll 1$.

It is expected that the printing parameters can be tuned to affect the fusion and therefore the contact resistance σ and, hence, Γ. The contact resistance is likely accounted for by voids, improper fusion or the distribution of conductive nanoparticles [3], [8], [26]. For a given material the nozzle temperature T_{noz} and the environment or bed temperature T_{bed} are crucial in the bond formation between lines [27], [28]. Higher temperatures in general give lower total resistance for 3D-prints [8], [29]. Furthermore the extrusion width W_{ext} determines the number of contacts for a fixed sample size, and increasing it is shown to minimize the total resistance in 3D-prints [6], [8]. Therefore the printing parameters under study are T_{noz}, T_{bed} and W_{ext}.

III. Methodology

A. Fabrication

The samples are single sheets fabricated with a Prusa i3 mk3s printer with a $0.4\,\mathrm{mm}$ nozzle, combined with PrusaSlicer for slicing. As material ProtoPasta conductive PLA is used [30]. The samples are squares of 30 x 30 x 0.2 mm, printed on top of oxidized silicon wafers, where a spray is used to improve adhesion (3DLAC). The electrical contacts are made with copper tape and silver paint (Electrolube SCP26G), having additional ridges on the outer ends of the samples to provide even contacts. For testing the effect of the print parameters on the anisotropy, prints are made with a $\phi = 45°$ infill angle, fig. 1.b. Two probing points are added symmetrically on either side for reliable voltage probing, fig. 1.b, where the average voltage difference of both pairs is used as measure for the anisotropic voltage distribution. The prints are made with the default printing parameters from table I, while varying a single parameter at a time: T_{noz} from $200\,°\mathrm{C}$ to $230\,°\mathrm{C}$, T_{bed} from $25\,°\mathrm{C}$ to $70\,°\mathrm{C}$ and W_{ext} $0.4\,\mathrm{mm}$ to $1.2\,\mathrm{mm}$. A concentrator consisting out of four combined versions of the sample in fig. 1.b is also fabricated as a metamaterial demonstration, on a glass and on a silicon wafer. The printing parameter values that yield the largest anisotropy are used to achieve a large contact resistance and hence the best metamaterial properties.

TABLE I
Default printing parameters

Printing parameter	Value
Bed temperature	$50\,°\mathrm{C}$
Nozzle temperature	$215\,°\mathrm{C}$
Extrusion width	$0.6\,\mathrm{mm}$
Extrusion multiplier	1
Infill Density	100%
Infill angle	$45°$
Layer height	$0.2\,\mathrm{mm}$
Printing speed	$20\,\mathrm{mm\,s^{-1}}$

B. Characterization

The resistance of the samples between the copper contacts and the voltage difference between opposite probe pairs are measured with a handheld digital multimeter (Fluke 170). For every parameter, 2 or 3 samples are tested. The cross sections of the samples with extreme parameters are imaged with a Leica Microsystems MSV266 microscope, where the cross-sections are prepared by cryo fracturing with liquid nitrogen. The concentrator demonstration is measured with IR thermography with an IR camera (FLIR ONE Gen 2, FLIR Systems) to show heating of the sample due to power dissipation. The temperature distribution is affected by thermal diffusion and convection, and therefore only serves as indicator for areas with high power density [7]. To show concentrating of the current, scanning probe voltage measurements are performed over the centerline of the concentrator with the multimeter.

FEM simulations are performed with COMSOL using the Electric Currents module with an extremely fine mesh. The electrical properties are implemented through material properties and contact impedance functionality, similar as in [7], [25]. The meandering ends of the lines are neglected, since these have a small effect for square samples with a relatively high Γ value [25]. The FEM simulations are compared to the voltage centerline measurements by means of fitting σ and by measuring $\rho = 0.221\,\Omega\,\mathrm{m}$ on a square sample along the print direction of the lines.

IV. Results

The mean results for the normalized voltage difference between the probes and the total resistance of the samples with the first standard deviation are shown in fig. 2, where every parameter has its own horizontal axis. As expected the voltage difference, and hence the anisotropy, goes down with increasing T_{noz}, T_{bed} and W_{ext}, indicating a decrease in contact resistance. The total resistance also goes down with an increase of these parameters, as already found in [6], [29]. This holds for all values except for the highest T_{noz} and T_{bed}, which does not have an explanation yet.

To validate that the difference in anisotropy is caused by the contact properties, microscopy images are taken of the samples with the highest and lowest value for each parameter, fig. 3.

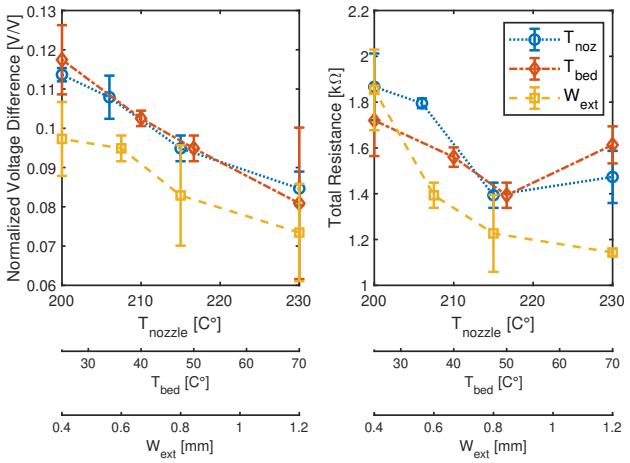

Fig. 2. The measured mean normalized voltage difference (left) and total resistance (right) with their standard deviation as a function of the parameters T_{noz}, T_{bed} and W_{ext}, where each parameter has an own horizontal axis.

For the low T_{noz}, T_{bed} improper fusion can be recognized, whereas for the high values the cross-sections appear solid. For the cross sections with varied W_{ext}, the contact areas have ridges for $W_{\text{ext}} = 0.4\,\text{mm}$ and gutters for $W_{\text{ext}} = 1.2\,\text{mm}$. This over and under-extrusion might explain the smaller effect on the voltage difference for W_{ext}.

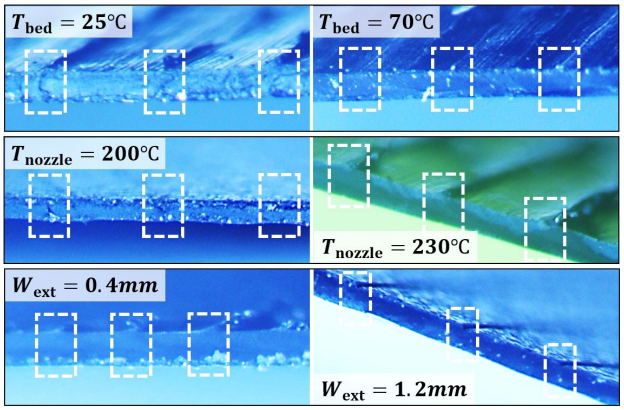

Fig. 3. Microscopy images of cross sections from samples with a single extreme parameter. The low temperatures show reduced bonding formation, compared to the fully fused contacts at high temperatures. The extrusion width seems to cause over and under-extrusion for low and high values.

The most effective parameters from fig. 2 are used for printing the concentrator: $T_{\text{noz}} = 200\,°\text{C}$, $T_{\text{bed}} = 25\,°\text{C}$ and $W_{\text{ext}} = 0.4\,\text{mm}$. The concentrator in fig. 4.a is measured with IR thermography, fig. 4.b and shows qualitatively comparable results to FEM simulations of the power dissipation density in fig. 4.c, showing its operation with heating mainly on the corners and in the center of the concentrator.

The scanning probe voltage measurements over the centerline in fig. 5 also show a higher voltage gradient in the center compared to a linear voltage drop for isotropic materials, demonstrating the concentrating effect. The FEM simulations are fitted to the measurements, yielding a $\Gamma = 0.570$ (Si) and $\Gamma = 0.307$ (glass), comparable to the anisotropy ratio of $\Gamma = 0.528$ in [7]. The difference between the samples on the glass and silicon wafers might be explained from the different thermal properties of the substrates, affecting bond formation.

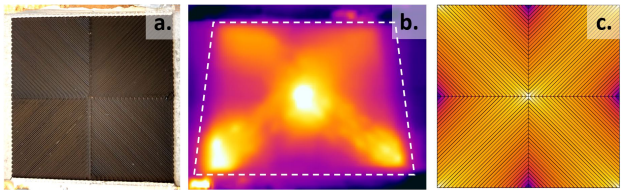

Fig. 4. **a.** The fabricated concentrator. **b.** An IR image of the concentrator in operation, mainly showing heating at the center and in the corners. **c.** A FEM simulation of the power dissipation density on a logarithmic scale, showing similarity to the IR measurement.

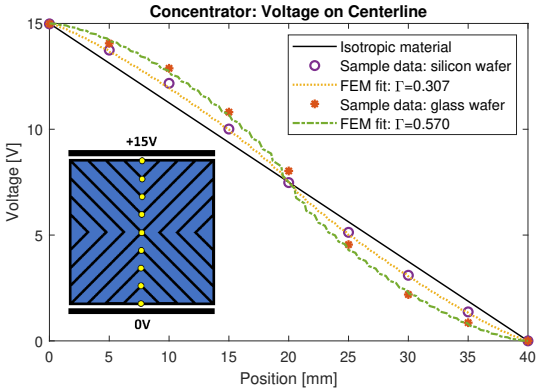

Fig. 5. The measured voltage and fitted simulations over the centerline of the fabricated concentrators, demonstrating its operation with a higher electric field in the middle. The concentrator is schematically shown on the left, with the dots representing the probe locations.

V. Discussion and Conclusions

This work proves experimentally that decreasing the nozzle temperature, bed temperature and extrusion width can be used to increase the contact resistance, to achieve anisotropic electrical conduction with FDM in single layer prints. Through microscopy it is validated that the printing parameters indeed influence the quality of the contacts between printed lines. The anisotropy is used for DC electric metamaterials, which are interesting for sensing e.g. by concentrating the current to increase sensitivity. Such a concentrator is 3D-printed and its operation is demonstrated through IR thermography and voltage measurements and compared with FEM simulations.

In this study a limited set of printing parameters is researched in a 2D case, leaving space for future studies. Furthermore it was observed that the extreme settings mechanically weaken the 3D-prints and make it more difficult to print. Printing with dual materials could remedy this aspect, allowing for full 3D geometries and improved mechanical performance.

Acknowledgment

The authors thank Riccardo Sneep for his support with 3D-printing.

REFERENCES

[1] Y. Xu, X. Wu, X. Guo, B. Kong, M. Zhang, X. Qian, S. Mi, and W. Sun, "The boom in 3d-printed sensor technology," *Sensors*, vol. 17, no. 5, 2017.

[2] A. Dijkshoorn, P. Werkman, M. Welleweerd, G. Wolterink, B. Eijking, J. Delamare, R. Sanders, and G. J. M. Krijnen, "Embedded sensing: integrating sensors in 3-d printed structures," *Journal of Sensors and Sensor Systems*, vol. 7, no. 1, pp. 169–181, 2018. [Online]. Available: https://jsss.copernicus.org/articles/7/169/2018/

[3] M. Schouten, G. Wolterink, A. Dijkshoorn, D. Kosmas, S. Stramigioli, and G. Krijnen, "A review of extrusion-based 3d printing for the fabrication of electro-and biomechanical sensors," *IEEE Sensors Journal*, pp. 1–1, 2020.

[4] B. Hampel, S. Monshausen, and M. Schilling, "Properties and applications of electrically conductive thermoplastics for additive manufacturing of sensors," *Technisches Messen*, vol. 84, no. 9, pp. 593–599, 2017.

[5] N. Lazarus and S. S. Bedair, "Creating 3d printed sensor systems with conductive composites," *Smart Materials and Structures*, vol. 30, no. 1, p. 015020, dec 2020. [Online]. Available: https://doi.org/10.1088/1361-665x/abcbe2

[6] J. Zhang, B. Yang, F. Fu, F. You, X. Dong, and M. Dai, "Resistivity and its anisotropy characterization of 3d-printed acrylonitrile butadiene styrene copolymer (abs)/carbon black (cb) composites," *Applied Sciences*, vol. 7, no. 1, 2017.

[7] A. Dijkshoorn, M. Schouten, G. Wolterink, R. Sanders, S. Stramigioli, and G. Krijnen, "Characterizing the electrical properties of anisotropic, 3d-printed conductive sheets for sensor applications," *IEEE Sensors Journal*, vol. 20, no. 23, pp. 14 218–14 227, 2020.

[8] F. Daniel, A. Gleadall, and A. D. Radadia, "Influence of interface in electrical properties of 3d printed structures," *Additive Manufacturing*, vol. 46, p. 102206, 2021.

[9] S. Mousavi, D. Howard, F. Zhang, J. Leng, and C. H. Wang, "Direct 3D Printing of Highly Anisotropic, Flexible, Constriction-Resistive Sensors for Multidirectional Proprioception in Soft Robots," *ACS Applied Materials and Interfaces*, vol. 12, no. 13, pp. 15 631–15 643, 2020.

[10] G. Wolterink, R. Sanders, and G. Krijnen, "Thin, flexible, capacitive force sensors based on anisotropy in 3d-printed structures," in *2018 IEEE SENSORS*, 2018, pp. 1–4.

[11] C. Navau, R. Mach-Batlle, A. Parra, J. Prat-Camps, S. Laut, N. Del-Valle, and A. Sanchez, "Enhancing the sensitivity of magnetic sensors by 3d metamaterial shells," *Scientific Reports*, vol. 7, 2017.

[12] H. Barati Sedeh, M. Fakheri, A. Abdolali, and F. Sun, "Experimental demonstration of an arbitrary shape dc electric concentrator," *Scientific Reports*, vol. 10, no. 1, 2020.

[13] T. Yang, X. Bai, D. Gao, L. Wu, B. Li, J. T. L. Thong, and C.-W. Qiu, "Invisible sensors: Simultaneous sensing and camouflaging in multiphysical fields," *Advanced Materials*, vol. 27, no. 47, pp. 7752–7758, 2015.

[14] T. Han and C.-W. Qiu, "Transformation laplacian metamaterials: recent advances in manipulating thermal and dc fields," *Journal of Optics*, vol. 18, no. 4, p. 044003, apr 2016.

[15] M. Kadic, T. Bückmann, R. Schittny, and M. Wegener, "Metamaterials beyond electromagnetism," *Reports on Progress in Physics*, vol. 76, no. 12, p. 126501, nov 2013. [Online]. Available: https://doi.org/10.1088/0034-4885/76/12/126501

[16] P. R. Bandaru, K. P. Vemuri, F. M. Canbazoglu, and R. S. Kapadia, "Layered thermal metamaterials for the directing and harvesting of conductive heat," *AIP Advances*, vol. 5, no. 5, p. 053403, 2015.

[17] W. Jiang, C. Luo, H. Ma, Z. Mei, and T. Cui, "Enhancement of current density by dc electric concentrator," *Scientific Reports*, vol. 2, 2012.

[18] F. Yang, Z. Mei, T. Jin, and T. Cui, "Dc electric invisibility cloak," *Physical Review Letters*, vol. 109, no. 5, 2012.

[19] T. Han, H. Ye, Y. Luo, S. P. Yeo, J. Teng, S. Zhang, and C.-W. Qiu, "Manipulating dc currents with bilayer bulk natural materials," *Advanced Materials*, vol. 26, no. 21, pp. 3478–3483, 2014. [Online]. Available: https://onlinelibrary.wiley.com/doi/abs/10.1002/adma.201305586

[20] M. Askari, D. A. Hutchins, P. J. Thomas, L. Astolfi, R. L. Watson, M. Abdi, M. Ricci, S. Laureti, L. Nie, S. Freear, R. Wildman, C. Tuck, M. Clarke, E. Woods, and A. T. Clare, "Additive manufacturing of metamaterials: A review," *Additive Manufacturing*, vol. 36, p. 101562, 2020. [Online]. Available: https://www.sciencedirect.com/science/article/pii/S2214860420309349

[21] X. Wu, Y. Su, and J. Shi, "Perspective of additive manufacturing for metamaterials development," *Smart Materials and Structures*, vol. 28, no. 9, p. 093001, aug 2019. [Online]. Available: https://doi.org/10.1088/1361-665x/ab2eb6

[22] T. Koschny, C. M. Soukoulis, and M. Wegener, "Metamaterials in microwaves, optics, mechanics, thermodynamics, and transport," *Journal of Optics*, vol. 19, no. 8, p. 084005, jul 2017.

[23] G. Park, S. Kang, H. Lee, and W. Choi, "Tunable multifunctional thermal metamaterials: Manipulation of local heat flux via assembly of unit-cell thermal shifters," *Scientific Reports*, vol. 7, 2017.

[24] R. H. Tarkhanyan and D. G. Niarchos, "Geometrically Tunable Transverse Electric Field in Multilayered Structures," *Advances in Condensed Matter Physics*, vol. 2017, 2017.

[25] A. Dijkshoorn, M. Schouten, S. Stramigioli, and G. Krijnen, "Modelling of anisotropic electrical conduction in layered structures 3d-printed with fused deposition modelling," *Sensors*, vol. 21, no. 11, 2021. [Online]. Available: https://www.mdpi.com/1424-8220/21/11/3710

[26] G. Stano, A. Di Nisio, A. Lanzolla, M. Ragolia, and G. Percoco, "Fused filament fabrication of commercial conductive filaments: experimental study on the process parameters aimed at the minimization, repeatability and thermal characterization of electrical resistance," *International Journal of Advanced Manufacturing Technology*, vol. 111, no. 9-10, pp. 2971–2986, 2020.

[27] C. Bellehumeur, L. Li, Q. Sun, and P. Gu, "Modeling of bond formation between polymer filaments in the fused deposition modeling process," *Journal of Manufacturing Processes*, vol. 6, no. 2, pp. 170–178, 2004.

[28] N. Polychronopoulos and J. Vlachopoulos, "The role of heating and cooling in viscous sintering of pairs of spheres and pairs of cylinders," *Rapid Prototyping Journal*, vol. 26, no. 4, pp. 719–726, 2020.

[29] H. Watschke, K. Hilbig, and T. Vietor, "Design and characterization of electrically conductive structures additively manufactured by material extrusion," *Applied Sciences*, vol. 9, no. 4, 2019.

[30] ProtoPlant, makers of Proto-pasta, "Composite PLA - Electrically Conductive Graphite." [Online]. Available: https://www.proto-pasta.com/